VERSITA

CELLULAR & MOLECULAR BIOLOGY LETTERS
Volume 11, (2006) pp 90 – 101
http://www.cmbl.org.pl

DOI: 10.2478/s11658-006-0009-3

Received: 08 September 2005
Revised form accepted: 06 January 2006

SHAPE VARIATION OF BILAYER MEMBRANE DAUGHTER VESICLES INDUCED BY ANISOTROPIC MEMBRANE INCLUSIONS

KLEMEN BOHINC[1,2], DARKO LOMBARDO[1], VERONIKA KRALJ-IGLIČ[1,3], MIHA FOŠNARIČ[1], SYLVIO MAY[4] , FRANJO PERNUŠ[1], HENRY HÄGERSTRAND[5] and ALEŠ IGLIČ[1]*

[1]Laboratory of Physics, Faculty of Electrical Engineering, University of Ljubljana, Tržaška 25, SI-1000 Ljubljana, Slovenia, [2]University College for Health Studies, University of Ljubljana, Poljanska 26a, SI-1000 Ljubljana, Slovenia, [3]Institute of Biophysics, Faculty of Medicine, University of Ljubljana, Lipičeva 2, 1000 Ljubljana, Slovenia, [4]Department of Physics, North Dakota State University, Fargo, ND 58105-5566, USA, [5]Department of Biology, Åbo Akademi University, Åbo/Turku, FIN-20520, Finland

Abstract: A theoretical model of a two-component bilayer membrane was used in order to describe the influence of anisotropic membrane inclusions on shapes of membrane daughter micro and nano vesicles. It was shown that for weakly anisotropic inclusions the stable vesicle shapes are only sligthly out-of-round. In contrast, for strongly anisotropic inclusions the stable vesicle shapes may significantly differ from spheres, i.e. they have a flattened oblate shape at small numbers of inclusions in the membrane, and an elongated cigar-like prolate shape at high numbers of inclusions in the vesicle membrane.

Key words: Bilayer membranes, Daughter vesicles, Anisotropic membrane inclusions

INTRODUCTION

Biological membranes can be viewed as a bilayer of lipid molecules into which other molecules such as membrane proteins and glycolipids are embedded [1, 2]. In the seventies, a theoretical model was proposed where the membrane was described as a two-dimensional liquid [1]. Accordingly the stable shapes of closed bilayer membranes were assumed to be determined by minimization of

* Corresponding author; e-mail: ales.iglic@fe.uni-lj.si

the isotropic membrane bending energy [5], i.e. the bending energy of a membrane composed of molecules which are considered as isotropic with respect to the axis pointing in the direction of the normal to the bilayer.

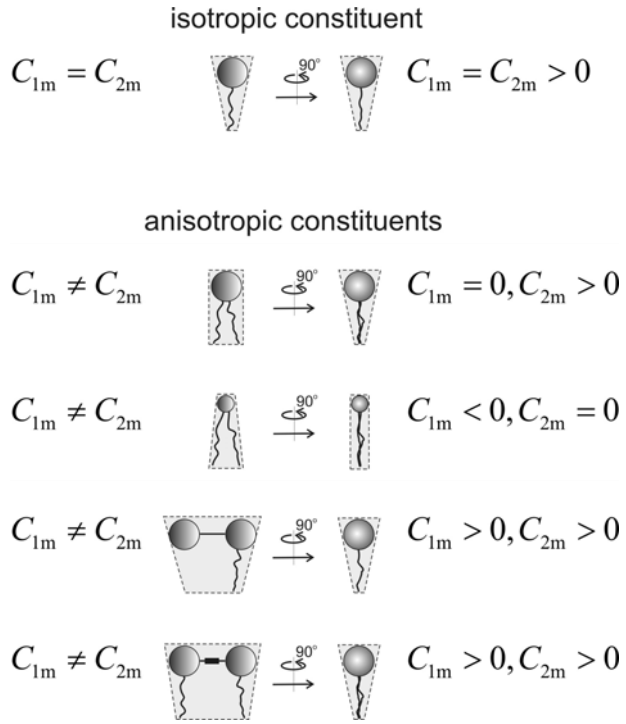

Fig. 1. Schematic representation of isotropic and anisotropic membrane constituents. Front and side views are shown. The principal curvatures C_{1m} and C_{2m} describe the intrinsic shape of the molecule. Gemini detergents (shown in the figure) are typical examples of a strongly anisotropic molecule composed of two head-tail entities that are joined by a spacer in the headgroup level [3, 4].

Recently, strong evidence has been accumulated which indicates that the single membrane constituents (Fig. 1), as well as the membrane inclusions (Fig. 2), are in general anisotropic [6, 7]. It was shown that anisotropic membrane inclusions, induced by exogeneously bound detergents, can strongly influence the shape of cells and the shape of cell membrane daughter micro and nanovesicles [6, 8, 9].
The influence of detergents on the shape of the membrane has also been studied in lipid vesicles. Recently Staneva et al. [10] investigated the effect of detergents on the shape and vesiculation (budding) of giant unilamellar vesicles. They showed that budding of the bilayer membrane may be induced by the initial incorporation of detergent in the outer membrane leaflet, increasing the local spontaneous curvature of the bilayer [11]. Budding and tubulation were

also studied in highly oblate phospholipid vesicles with anchored polymers or oleoylcoenzyme A [12], where the concentration of the anchors (i.e. membrane inclusions) seems to be the dominant parameter in determining the amount of induced membrane curvature.

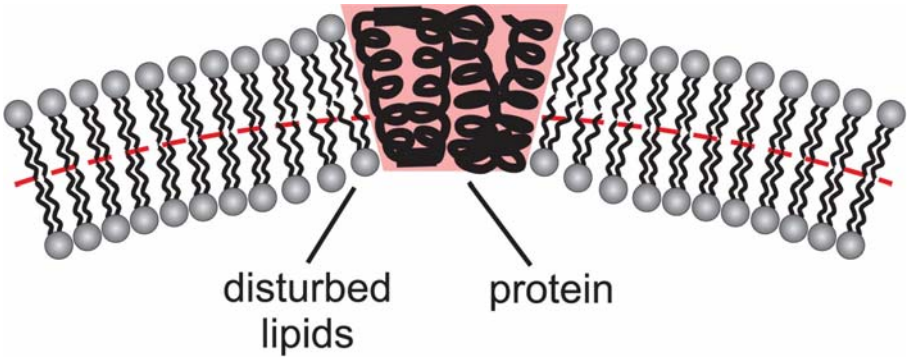

Fig. 2. Schematic figure of a single protein membrane inclusion. Note that the intrinsic shape of the protein inclusion, characterized by intrinsic curvatures C_{1m} and C_{2m}, differs from the real (geometrical) shape of the protein. Intrinsic curvatures C_{1m} and C_{2m} are the principal curvatures of the membrane which corresponds to the minimal possible energy of the protein inclusion and the surrounding disturbed lipids (E_{min}). The binding of detergents on the membrane protein (see also [13]) may change the values of C_{1m} and C_{2m}.

The anisotropic membrane components or inclusions interact with the anisotropically curved membrane bilayer (regions of the membrane where the principal curvatures are different) in an orientation dependent manner and thus contribute to the deviatoric energy [14, 15] of the membrane. These anisotropic membrane inclusions can move laterally over the phospholipid layer and also rotate around their axes normal to the membrane. They can take the energetically most favourable place and orientation in the membrane. In this way the anisotropic membrane inclusions may considerably influence the membrane elastic free energy and the corresponding equilibrium shapes of the membrane [16, 17].

In the eighties Markin [18] was the first to develop a theoretical model for the determination of erythrocyte shape transformations and the distribution of membrane components over the membrane surface. The Markin theoretical model is based on the concept of the fluid mosaic model. The free energy of a membrane composed of two species of molecules was derived by employing the spontaneous curvature model where, in addition to the membrane isotropic bending energy, the energy contributions due to the membrane components were included. The influence of membrane components on the membrane spontaneous curvature and curvature elasticities were also taken into account. Markin showed that a nonuniform organization of different components over the

membrane may arise. He also studied how the distribution of membrane components affects the membrane shape.

In this work, stable shapes of daughter vesicles of a bilayer membrane with inclusions corresponding to the minimum of the membrane free energy and the corresponding lateral distribution of membrane components were studied theoretically. The vesicle membrane was assumed to be composed of two kinds of molecules: phospholipid molecules and anisotropic membrane inclusions. For the sake of simplicity, the anisotropic phospholipid molecules were taken to be isotropic. The model of a two-component bilayer membrane was used to study the dependence of equilibrium shapes of the bilayer membrane daughter micro and nanovesicles as a function of the number and intrinsic shape of the membrane inclusions.

THEORY AND RESULTS

Since the thickness of the bilayer membrane is much smaller than the dimensions of the membrane in the lateral direction, the bilayer membrane resembles a two dimensional surface in a three dimensional space. At a chosen point on the two dimensional surface we cut the surface by a plane through the normal to the surface. The intersection forms a curve in space, the so-called normal cut. The inverse of the radius of the circle that fits the normal cut at the chosen point is by definition the curvature of the normal cut at the chosen point. If from all possible normal cuts we choose those with extreme curvatures, we find that these are the principal curvatures C_1 and C_2 of the two dimensional membrane surface at a chosen point.

In the model, the membrane is composed of two kinds of constituents; phospholipid molecules and anisotropic membrane inclusions. The anisotropic inclusions have principal curvatures $C_{1m,1}$ and $C_{2m,1}$ which describe their intrinsic shapes. Our description of the two-component bilayer membrane starts from a microscopic description of the membrane constituents. We take into account the deviatoric energy of the membrane which is based on the orientational ordering of the anisotropic membrane constituents [6, 16], where the relative orientation of the anisotropic inclusions influences the free energy of the membrane. The free energy was expressed by two local invariants: the mean curvature $H = (C_1 + C_2)/2$ and the curvature deviator $D = |C_1 - C_2|/2$ [14-16].

The membrane inclusions with average area density fraction $\overline{m}_1$ have an intrinsic mean curvature $H_{m,1} = (C_{1m,1} + C_{2m,1})/2$ and an intrinsic curvature deviator $D_{m,1} = (C_{1m,1} - C_{2m,1})/2$. The isotropic lipid molecules have equal principal curvatures ($C_{1m,2} = C_{2m,2}$), the mean curvature is $H_{m,2} = C_{1m,2}$ and the intrinsic curvature deviator is $D_{m,2} = 0$ [15, 17]. In the limit of small area density fractions $m_1 << 1$, $\overline{m}_1 << 1$ and strong interaction $(K_1 >> K_2, |\overline{K}_1| >> |\overline{K}_2|)$, the free energy of the membrane monolayer (ΔF) is given by [14]:

$$\Delta F = NkT\left[\frac{1}{A}\int g_2 dA - \overline{m}_1 \ln\left(\frac{1}{A}\int e^{\Delta g} I_0(2\overline{K}_1 DD_{m,1})dA\right)\right], \qquad (1)$$

where $\Delta g = g_2 - g_1$ with $g_i = (2K_i + \bar{K}_i)(H^2 - 2HH_{m,i}) - \bar{K}_i D^2; i \in \{1,2\}$, where K_i and $\overline{K}_i$ are interaction constants [14], i = 1 denotes anisotropic inclusions, i = 2 isotropic phospholipid molecules, $\overline{m}_1$ the average area density fraction of anisotropic inclusions, dA the infinitesimal area element, A the membrane area, N the total number of molecules in one monolayer and I_0 the modified Bessel function. The second term in Eq. 1 describes the deviatoric energy.

We restricted our analysis of stable shapes of cell membrane daughter vesicles to ellipsoidal vesicle shapes with rotational symmetry around the z axis (Fig. 3). The main semi-axes of the ellipsoid are R and B. The azimuthal angle ϑ measures the angular distance from the x axis (in the positive and in the negative direction). The mean curvature H and the curvature deviator D of the ellipsoid with rotational symmetry around z axis can be written as:

$$H = \frac{B(2R^2 + (B^2 - R^2)\cos^2\vartheta)}{2R(R^2\sin^2\vartheta + B^2\cos^2\vartheta)^{3/2}}, \quad D = \frac{B(B^2 - R^2)\cos^2\vartheta}{2R(R^2\sin^2\vartheta + B^2\cos^2\vartheta)^{3/2}}. \qquad (2)$$

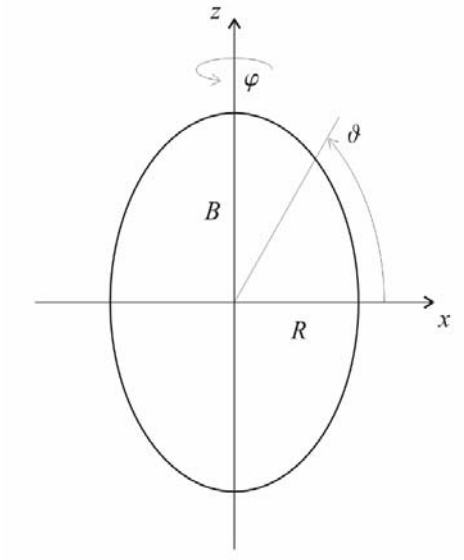

Fig. 3. Schematic representation of an ellipsoid with rotational symmetry around the z axis. The main semiaxes are R and B.

Two types of ellipsoidal vesicles are considered: the prolate (elongated) ellipsoid with $B > R$, and the oblate ellipsoid with $B < R$. The semiaxis B can be expressed as $B = R(1+\delta)$, where the parameter δ is positive for a prolate ellipsoid ($\delta > 0$) and negative for an oblate ellipsoid ($-1 < \delta < 0$). The area of the prolate ellipsoid with rotational symmetry is

$$A = 2\pi R^2 \left(1 + \frac{B}{R} \cdot \frac{\arcsin\sqrt{1-\frac{R^2}{B^2}}}{\sqrt{1-\frac{R^2}{B^2}}} \right), \qquad (3)$$

while the area of the oblate ellipsoid with rotational symmetry is

$$A = 2\pi R^2 \left(1 + \frac{B}{R} \cdot \frac{\operatorname{arsh}\sqrt{\frac{R^2}{B^2}-1}}{\sqrt{\frac{R^2}{B^2}-1}} \right). \qquad (4)$$

The total free energy of the membrane is the sum of the free energy contributions of the outer layer composed of isotropic lipid molecules and anisotropic inclusions, and of the inner layer composed of isotropic lipid molecules only. The absolute minimum of the membrane free energy ΔF corresponding to the equilibrium shape of the vesicle was searched for given the values of membrane area A, intrinsic mean curvature ($H_{m,1}$), curvature deviator ($D_{m,1}$) and average area density fraction of the inclusions $\overline{m}_1$. A constant area of the vesicle A was used as a constraint.

The results of this minimization procedure (Fig. 4), i.e. the equilibrium vesicle shapes in the ($D_{m,1}$, $\overline{m}_1$) space, are presented in Fig. 5. It can be seen in Fig. 5 that for weakly anisotropic inclusions (small $D_{m,1}$) the stable vesicle shapes are nearly spherical. On the other hand, the stable vesicles may significantly differ from spheres for strongly anisotropic membrane inclusions (large $D_{m,1}$). They have a flattened oblate shape at a small number of anisotropic inclusions in the membrane (small $\overline{m}_1$) and an elongated cigar-like prolate shape at a high number of anisotropic inclusions (large $\overline{m}_1$) in the vesicle membrane.

Discontinuous transitions between different classes of vesicle shapes can be observed in Figs. 4 and 5. The upper graph in Fig. 5 shows the ratio between the semiaxes of an ellipsoidal vesicle as a function of the intrinsic curvature deviator $D_{m,1}$ for different average fractions of the area density $\overline{m}_1$. The straight line at $\frac{B}{R} = \frac{R}{B} = 1$ corresponds to the sphere ($\overline{m}_1 = 0$). At constant $\overline{m}_1$, the ratio B/R continuously increases with increasing $D_{m,1}$ and then reaches the maximal ratio B/R before the discontinuous transition occurs. In the case of small

$\overline{m}_1 < 0.02$, a discontinuous transition from prolate to oblate ellipsoidal shape occurs. After this transition the ratio R/B increases with increasing $D_{m,1}$. At high $\overline{m}_1 > 0.02$, a discontinuous transition between the weak and the pronounced prolate ellipsoidal vesicle as well as a discontinuous transition between the pronounced prolate and the oblate ellipsoidal vesicle takes place.

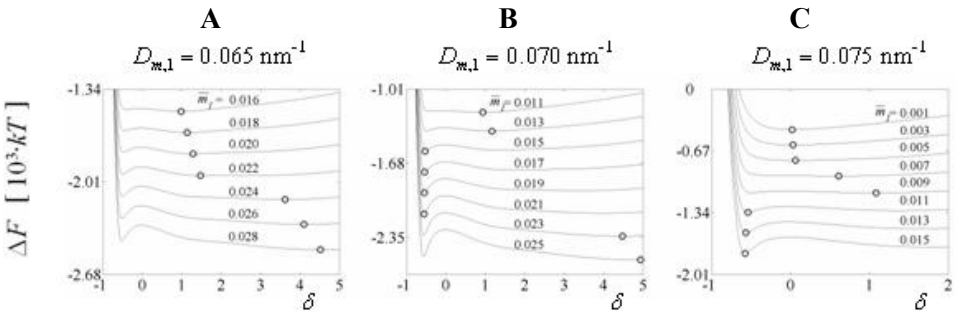

Fig. 4. Free energy of the membrane as a function of the parameter δ. Stable states corresponding to global minima are denoted by circles. In discontinuous transitions there is a jump in the position of the global minimum, while in continuous transitions the local minimum moves continuously; A - a continuous transition from sphere to prolate shape and a discontinuous transition from the prolate shape to the pronounced prolate shape, B - a continuous transition from sphere to prolate shape, a discontinuous transition from prolate shape to oblate shape and a discontinuous transition from oblate shape to pronounced prolate shape, and C - a continuous transition from sphere to prolate shape and a discontinuous transition from prolate shape to oblate shape.

Fig. 4 shows the membrane free energy as a function of parameter δ for some chosen values of $D_{m,1}$ and $\overline{m}_1$. The global minima at given $D_{m,1}$ and $\overline{m}_1$ are indicated by circles. Fig. 4C shows the continuous transition, i.e. the movement of the local minimum, from the spherical shape to the prolate ellipsoidal shape and the discontinuous transition from the prolate to the oblate ellipsoidal shape when a new local minimum at lower δ becomes the global minimum. Additionally, Fig. 4B shows the discontinuous transitions from the oblate to a pronounced prolate shape with formation of the third local minimum at higher average area density fractions $\overline{m}_1$. At lower intrinsic deviators $D_{m,1} < 0.067$ nm^{-1} the second local minimum (at $\delta < 0$) never becomes the global minimum and only discontinuous transitions from the prolate to the pronounced prolate ellipsoidal shape can be observed as shown in Fig. 4A. As we see in Fig. 4, typical absolute values of the free energies are a few thousand kT.

CONCLUSION

In this work the role of anisotropic membrane inclusions in determination of stable shapes of membrane daughter vesicles was studied. The equilibrium vesicle shapes were determined by minimization of the bilayer membrane free energy consisting of bending and deviatoric parts. It was shown theoretically that for weakly anisotropic inclusions the stable vesicle shapes are nearly spherical, while for strongly anisotropic membrane inclusions the stable vesicle shapes may significantly differ from spheres. They may have a flattened oblate shape at small number of inclusions and an elongated cigar-like prolate shape at high number of inclusions in the vesicle membrane (Fig. 5).

The calculated equilibrium shapes were obtained for the model system of bilayer membrane vesicles with anisotropic inclusions. We have discussed the relationship between these theoretically predicted shapes and the observed membrane daughter vesicle shapes in biological systems [8, 9, 15, 17]. Similar shapes of membrane daughter vesicles to those predicted in Fig. 5 have been observed in the erythrocyte membrane (Fig. 6) [5, 9, 19-21]. It was observed that amphiphile-induced microexovesicles of the erythrocyte membrane may be spherical or cylindrical, depending on the species of the added amphiphile. Predominantly spherical microexovesicles were released to the outer solution by dodecyltrimethylammonium bromide or dodecylzwittergentom (Fig. 6B), which are examples of weakly anisotropic inclusions. Tubular microexovesicles were released by dodecyl D-maltoside (Fig. 6A) [22] or dimeric dioctyldiQAS [15], which are examples of strongly anisotropic inclusions. Further, in human erythrocytes polyoxyethyleneglycolalkylether induces a large oblate torocyte-like endovesicle [17]. Qualitatively, these experimental results could be connected to the results of our calculations (Fig. 5), where spherical, oblate (flattened) and prolate (long tubular) shapes of the membrane were obtained. Tubular structures [22] could be linked to the calculated prolate ellipsoidal vesicle shape of the ellipsoid, while torocyte-like vesicles [17] could be linked to the calculated oblate ellipsoidal vesicle shape.

Anisotropic inclusions with a large intrinsic curvature deviator $D_{m,1}$ favour vesicle shapes with regions having a high curvature deviator D and in the case of flattened oblate vesicle shapes are predominantly distributed at small angles ϑ (see Fig. 3), i.e. at the highly curved vesicle rim where the membrane has a large curvature deviator D. In the central region at angles ϑ close to $\pi/2$, where the curvature deviator D of the flattened oblate vesicles is small, the area density of anisotropic inclusions is very small.

We analyzed the dependence of the membrane free energy on the parameter δ, the average area density fraction of anisotropic inclusions $\overline{m}_1$ and the intrinsic curvature deviator $D_{m,1}$ (Fig. 4). The energy of the transition from prolate shape to oblate shape is given by the difference between the free energies of the prolate

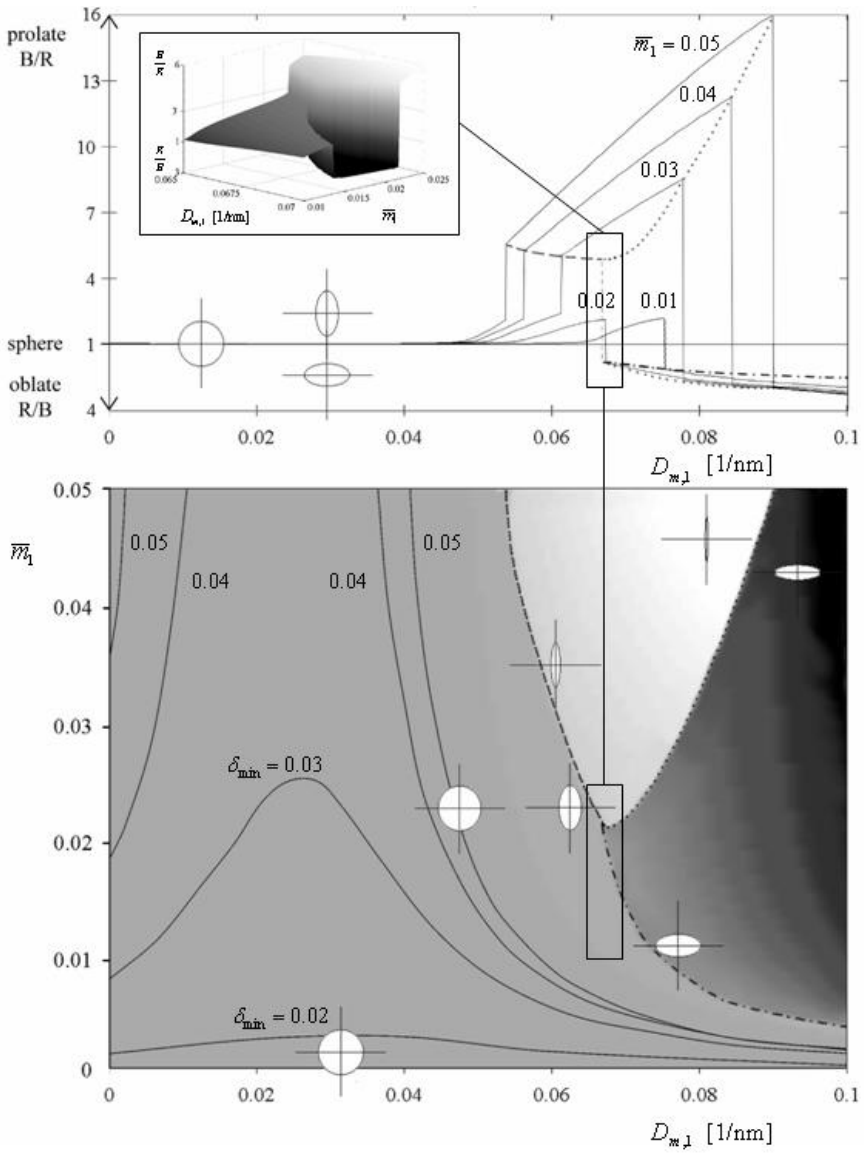

Fig. 5. Phase diagram of membrane daughter vesicle shapes in ($D_{m,1}$, $\overline{m}_1$) space. The regions of stable spherical and prolate (gray, $B/R > 1$), pronounced prolate (lighter, $B/R >> 1$) and oblate (darker, $B/R < 1$ i.e. $R/B > 1$) ellipsoidal vesicle shapes are indicated. Dashed, dotted and dashed-and-dotted lines represent discontinuous transitions from prolate to pronounced prolate, from oblate to pronounced prolate and from prolate to oblate ellipsoidal vesicle shapes, respectively. The model parameters are $H_{m,2} = 2/R_0$, $D_{m,2} = 0$, $K_1 = 600\,\mathrm{nm}^2$, $\overline{K}_1 = -400\,\mathrm{nm}^2$, $K_2 = 6\,\mathrm{nm}^2$, $\overline{K}_2 = -4\,\mathrm{nm}^2$, $H_{m,1} = D_{m,1}$ and $R_0 = 40\,\mathrm{nm}$.

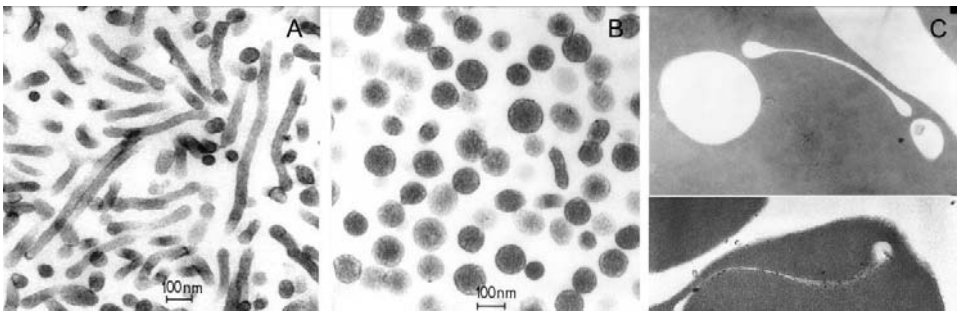

Fig. 6. Prolate tubular (A) [8, 20], spherical (B) and oblate (C) [17] daughter vesicles of the erythrocyte membrane.

and oblate shapes, while the energy barrier is given by the difference between the free energy of the prolate shape and the local maximum between the two shapes. As shown in Fig. 4, for a given intrinsic curvature deviator $D_{m,1}$ of the inclusions, the transition energy and the energy barrier increase with increasing average area density fraction $\overline{m}_1$. This increase is the result of the increase of the average concentration of inclusions, which prefer more curved regions of the membranes. The maximal energy of transition from the prolate shape to the oblate shape is approx. 175 kT for inclusions with an intrinsic deviator of 0.070 nm^{-1}. The maximal energy barrier is approx. 300 kT. The thermal fluctuation energy [23] can be estimated to lie between 50 kT and 500 kT for bending rigidities between 10^{-20}J and 10^{-19}J. This estimate of the fluctuation energy hints that transitions with small transition energy are not stable. Similar transition energies (up to 500 kT) were obtained by Kralj-Iglič et al. [21], where the transition between prolate and oblate discoid vesicles with embedded isotropic inclusions was studied. The main difference between the results of our calculation and the calculation of Kralj-Iglič et al. [21] is that we also obtained discontinuous transitions between oblate, prolate and pronounced prolate shapes.

To conclude, we suggested a model of a two-component bilayer membrane which considers the bilayer membrane as a two component system of isotropic lipids and anisotropic membrane inclusions. This model was used to study the interdependence between the membrane shape and the distribution of anisotropic inclusions for different intrinsic shapes of the anisotropic inclusions. Our model could also be used in description of the shape transitions of lipid vesicles in an electric [24] and a magnetic field [5] in order to study simultaneously the effect of both; intrinsic shape of anisotropic molecules and the electric/magnetic field on shape transitions.

REFERENCES

1. Singer, S.J. and Nicholson, G.L. The fluid mosaic model of the structure of cell membranes. **Science** 175 (1972) 720-731.
2. Israelachvili, J.N. **Intermolecular and surface forces.** Academic Press Limited, London, (1997).
3. Fisicaro, E. Gemini surfactants: Chemico-physical and biological properties. **Cell. Mol. Biol. Lett.** 2 (1997) 45-63.
4. Danino, D., Talmon, Y. and Zana, R. Vesicle-to-micelle transformation in systems containing dimeric surfaces. **J. Coll. Inter. Sci.** 185 (1997) 84-93.
5. Helfrich, W. Elastic properties of lipid bilayers: Theory and possible experiments. **Z. Naturforsch.** 28 (1973) 693-703.
6. Iglič, A. and Kralj-Iglič, V. **Planar Lipid Bilayers (BLMs) and Their Applications,** in: (Tien, H.T. and Ottova-Leitmannova, A. Eds). Membrane Science and Technology, Vol. 7 Elsevier Science B.V., Amsterdam, New York, chapter 4 (2003) 143-172.
7. Fournier, J.B. Nontopological saddle-splay and curvature instabilities from anisotropic membrane inclusions. **Phys. Rev. Lett.** 76 (1996) 4436–4439.
8. Hägerstrand, H. and Isoma, B. Vesiculation induced by amphiphiles in erythrocytes. **Biochim. Biophys. Acta** 982 (1989) 179-186.
9. Hägerstrand, H. and Isoma, B. Morphological characterization of exovesicles and endovesicles released from human erythrocytes following treatment with amphiphiles. **Biochim. Biophys. Acta** 1109 (1992) 117-126.
10. Staneva, G., Seigneuret, M., Koumanov, K., Trugnan, G. and Angelova, M.I. Vectorial budding of vesicles by asymmetrical enzymatic formation of ceramide in giant liposomes. **Chem. Phys. Lipids** 136 (2005) 55-66.
11. Iglič, A. and Hägerstrand, H. Amphiphile-induced spherical microexovesicle corresponds to an extreme local area difference between two monolayers of the membrane bilayer. **Med. Biol. Eng. Comp**. 37 (1999) 125-129.
12. Tsafrir, I., Caspi, Y., Guedeau-Boudeville, M.A., Arzi, T. and Stavans, J. Budding and tubulation in highly oblate vesicles by anchored amphiphilic molecules. **Phys. Rev. Lett.** 91 (2003) 138102-1-4.
13. Sjögren, H., Ericsson, C.A., Evenäs, J.and Ulvenlund, S. Interaction between charged polypeptides and nonionic surfactant. **Biophys. J.** 89 (2005) 4219-4233.
14. Kralj-Iglič, V., Heinrich, V., Svetina, S. and Žekš B. Free energy of closed membrane with anisotropic inclusions. **Eur. Phys. J. B** 10 (1999) 5-8.
15. Kralj-Iglič, V., Iglič, A., Hägerstrand, H. and Peterlin, P. Stable tubular microexovesicles of the erythrocyte membrane induced by dimeric amphiphiles. **Phys. Rev. E** 61 (2000) 4230–4234.
16. Iglič, A., Fošnarič, M., Hägerstrand, H. and Kralj-Iglič, V. Coupling between vesicle shape and the non-homogeneous lateral distribution of membrane constituents in Golgi bodies. **FEBS Lett**. 574 (2004) 9-12.

17. Hägerstrand, H., Kralj-Iglič, V., Fošnarič, M., Bobrowska- Hägerstrand, M., Mrówczyńska, L., Söderström, T. and Iglič, A., Endovesicle formation and membrane perturbation induced by polyoxyethylene- glycolalkylethers in human erythrocytes. **Biochim. Biophys. Acta** 1665 (2004) 191-200.
18. Markin, V.S. Lateral organization of membranes and cell shapes. **Biophys. J.** 36 (1981) 1-19.
19. Huttner, W.B. and Zimmerberg, J. Implications of lipid microdomains for membrane curvature, budding and fission-commentary. **Curr. Opin. Cell Biol.** 13 (2001) 478-484.
20. Kralj-Iglič, V., Iglič, A., Hägerstrand, H. and Bobrowska- Hägerstrand, M. Hypothesis of nanostructures of cell and phospholipid membranes as cell infrastructure. **Med. Razgl.** 44 (2005) 155-169.
21. Kralj-Iglič, V., Svetina, S. and Žekš, B. Shapes of bilayer vesicles with membrane embedded molecules. **Eur. Biophys. J.** 24 (1996) 311-321.
22. Hägerstrand, H., Kralj-Iglič, V., Bobrowska- Hägerstrand, M. and Iglič, A. Membrane skeleton detachment in spherical and cylindrical microexovesicle. **Bull. Math. Biol.** 61 (1999) 1019-1030.
23. Seifert, U. Configuration of fluid membranes and vesicles. **Adv. Phys.** 46 (1997) 13-137.
24. Helfrich, W. Deformation of lipid bilayer spheres by electric fields. **Z. Naturforsch.** 29c (1974) 182-183.